Inorganic Chemistry Communications 93 (2018) 65–68

Contents lists available at ScienceDirect

Inorganic Chemistry Communications

journal homepage: www.elsevier.com/locate/inoche

Short communication

Photocatalytic degradation of methyl orange by $BiOI/Bi_4O_5I_2$ microspheres under visible light irradiation

Xujing Xiao[a], Ying Lin[a], Bole Pan[c], Wenjie Fan[d], Yongchao Huang[a,b,*]

[a] School of Chemistry, Sun Yat-Sen University, 135 Xingang West Road, Guangzhou 510275, China
[b] Key Laboratory for Water Quality and Conservation of the Pearl River Delta, Ministry of Education, Research Institute of Environmental Research at Greater Bay, Guangzhou University, Guangzhou 510006, China
[c] Guangzhou Tianhe Foreign Language School, Guangzhou, China
[d] Analysis and Testing Center, South China Normal University, Guangzhou 510006, China

GRAPHICAL ABSTRACT

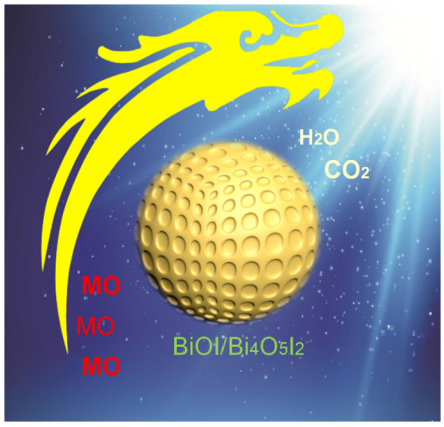

ARTICLE INFO

Keywords:
$BiOI/Bi_4O_5I_2$
Photocatalysis
Visible light
Methyl orange

ABSTRACT

$BiOI/Bi_4O_5I_2$ composites were synthesized by calcinations with BiOI microspheres at 400 °C. The $BiOI/Bi_4O_5I_2$ composites demonstrate 5 times higher photocatalytic activity than the pristine BiOI for methyl orange (MO) degradation under the irradiation of visible light. Moreover, the $BiOI/Bi_4O_5I_2$ composites have superior cycling stability. Such enhanced photoactivity is due to the significantly enhanced separation efficiency of photo-generated.

Photocatalysis has been used to remove the organic contaminants in wastewater [1–3]. Among the visible light active Bi-based photocatalysts, BiOI has the smallest band gap (1.6–1.9 eV) and unique structure (layered crystal structure consisting of $[Bi_2O_2]^{2+}$ layers sandwiched between two slabs of halogen ions) [4]. This structure can effectively generate more photocatalytic electrons and holes, which is benefited to the photocatalytic performances for degradation of the RhB and methyl orange (MO). However, low efficiency of photogenerated charge carriers limits its practical application [5,6].

Heterojunction, doping, and defect construction have been

* Corresponding author at: Key Laboratory for Water Quality and Conservation of the Pearl River Delta, Ministry of Education, Research Institute of Environmental Research at Greater Bay, Guangzhou University, Guangzhou 510006, China.
E-mail address: huangych@gzhu.edu.cn (Y. Huang).

https://doi.org/10.1016/j.inoche.2018.05.009
Received 25 April 2018; Received in revised form 3 May 2018; Accepted 8 May 2018

performed to improve the photocatalytic performance of BiOI [7–9]. Formation of heterojunctions could significantly enhance the separation of photogenerated charge carriers and the composites are photocatalytically more active than the individual components [10], such as Pd/BiOI/MnOx [11], $Bi_2S_3/Bi_2O_3/Bi_2O_2CO_3$ [12], $BiOI@Bi_{12}O_{17}Cl_2$ [13]. However, using one photocatalyst as a substrate and loading another photocatalyst onto the surface of the former will make the solid-solid contact interface unstable. This shortcoming leads to the difficulties of photoelectrons transport between two catalysts. Therefore, it is urgent to find a simple method to consolidate the interface inside the catalysts.

Calcination is extensively applied for constructing two phase contact interface. This will consolidate the interface, improving the photocatalytic performance [14,15]. For example, Cai et al. calcined $Bi_2O_2CO_3$ to form $Bi_2O_2CO_3/Bi_2O_3$ p-n heterojunction and they found that $Bi_2O_3/Bi_2O_2CO_3$ photocatalyst displayed much higher photocatalytic performance for the degradation of methylene blue than pure $Bi_2O_2CO_3$ and Bi_2O_3 under visible light [14]. These features inspired us to improve the photoactivity of BiOI by calcining BiOI to form BiOI/$Bi_4O_5I_2$ composites. The BiOI/$Bi_4O_5I_2$ composites demonstrate 5 times higher photocatalytic activity than the pristine BiOI for MO degradation under the irradiation of visible light. Moreover, the BiOI/$Bi_4O_5I_2$ composites have superior cycling stability. Such enhanced photoactivity is due to the significantly enhanced separation efficiency of photogenerated.

The BiOI/$Bi_4O_5I_2$ composites were obtained by annealing the pristine BiOI at 400 °C in air, which is according to the TG result (Fig. S1). As displayed in Fig. 1, BiOI and BiOI/$Bi_4O_5I_2$ composites consist of many microspheres self- assembled by nanosheets. SEM results reveal that morphology of microsphere has no change after thermal treatment. The detailed structure information of BiOI/$Bi_4O_5I_2$ composites is further studied by transmission electron microscopy (TEM). The images demonstrate that BiOI/$Bi_4O_5I_2$ composites appearance with microsphere-like (1.5 μm) and the microsphere composed of nanosheets. High-resolution TEM image of BiOI/$Bi_4O_5I_2$ displays that some interplanar distance of 0.30 nm and 0.317 nm appearance, which are corresponding to (102) plane of BiOI and (111) plane of $Bi_4O_5I_2$, respectively [16]. This result suggests that BiOI/$Bi_4O_5I_2$ composite is obtained after annealing BiOI at 400 °C in air.

The crystal structures of BiOI and BiOI/$Bi_4O_5I_2$ are analyzed by X-ray diffraction (XRD), which is displayed in Fig. 2a. The peaks of BiOI could be assigned to tetragonal BiOI (PCPDF no.: 10-0445) [17]. While some other peaks appear in the BiOI/$Bi_4O_5I_2$ spectra and could be designated to $Bi_4O_5I_2$ accordingly to the previously reported data [18]. Furthermore, Raman spectra are also carried out to identify the structure of BiOI/$Bi_4O_5I_2$ composites (Fig. 2b). The peaks at 85 cm^{-1} and 147 cm^{-1} are attributed to the Bi—I vibration of BiOI [19]. And the peaks at 300–600 cm^{-1} are due to the change of Bi—O environment. Therefore, the above results also confirm the successful formation of BiOI/$Bi_4O_5I_2$ composites. The electrochemical impedance spectra are performed to study the interface charge separation efficiency under the visible light irradiation and dark (Fig. 2c). The arc radius is smaller, meaning the efficiency of charge transfer is higher [20,21]. Thus, BiOI/$Bi_4O_5I_2$ has the highest charge transfer efficiency among the samples under the visible light irradiation. The fast charge transfer rate of BiOI/$Bi_4O_5I_2$ composites are attributed to the heterojunction, promoting the separation of electrons and holes. Furthermore, as displayed in Fig. S2, The absorption band gap of BiOI/$Bi_4O_5I_2$ shows blue shift compared to the pristine BiOI, revealing that BiOI could utilize more solar light. Undoubtedly, the enhanced photocatalytic activity of BiOI/$Bi_4O_5I_2$ sample cannot be due to the absorbing abilities.

The photocatalytic activity of BiOI and BiOI/$Bi_4O_5I_2$ are evaluated by degradation of MO with irradiation of visible light ($\lambda > 420$ nm). Fig. 3a shows the photocatalytic performance of degradation of MO over BiOI and BiOI/$Bi_4O_5I_2$. The absorption abilities of MO on BiOI and BiOI/$Bi_4O_5I_2$ in darkness are performed before the light on. BiOI sample and TiO_2 show weak photocatalytic performances, and only 40% and 12.2% of MO are degraded within 2 h, respectively. Comparatively, BiOI/$Bi_4O_5I_2$ presents a high photocatalytic activity with a degradation efficiency of 99%. Furthermore, the pseudo-first-order kinetics of BiOI and BiOI/$Bi_4O_5I_2$ are revealed according to Fig. 3a. The apparent rate constant of BiOI/$Bi_4O_5I_2$ (0.044 min^{-1}) is 11 times higher than that of BiOI (0.004 min^{-1}), revealing the excellent photocatalytic activity of BiOI/$Bi_4O_5I_2$ sample. Notably, after 6 successive cycles, the photocatalytic performance only slightly decreased under visible light, confirming the high stability of BiOI/$Bi_4O_5I_2$ (Fig. 3c). Furthermore, the BiOI/$Bi_4O_5I_2$ could also remove other dye pollutants such as RhB, methyl blue (MB), acid orange (AO), phenol and Congo red (CR), which could remove > 95% of these dyes after 120 min (Fig. 3d). All the above results demonstrate that BiOI/$Bi_4O_5I_2$ is a good photocatalyst

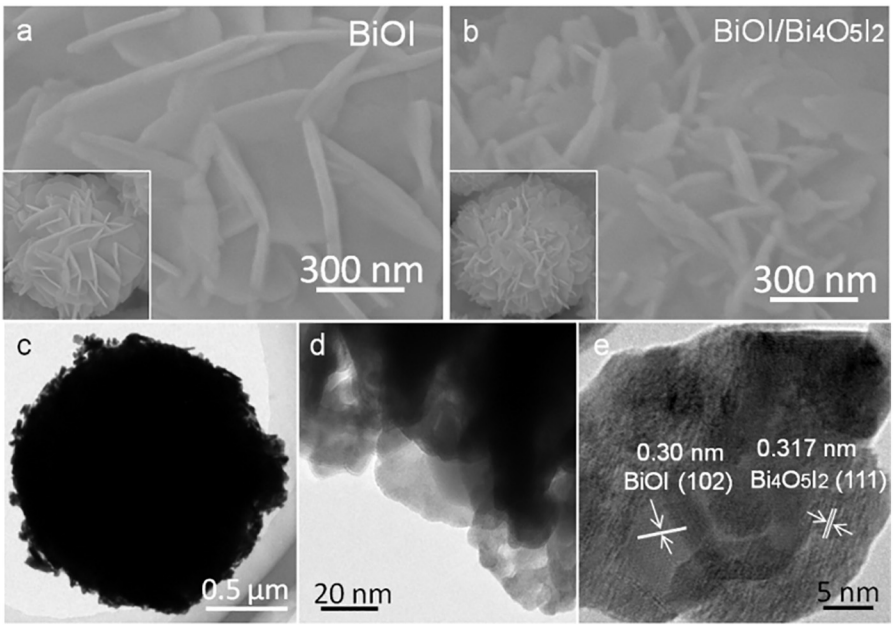

Fig. 1. SEM images of (a) BiOI and (b) BiOI/$Bi_4O_5I_2$. TEM images of BiOI/$Bi_4O_5I_2$ (c, d and e).

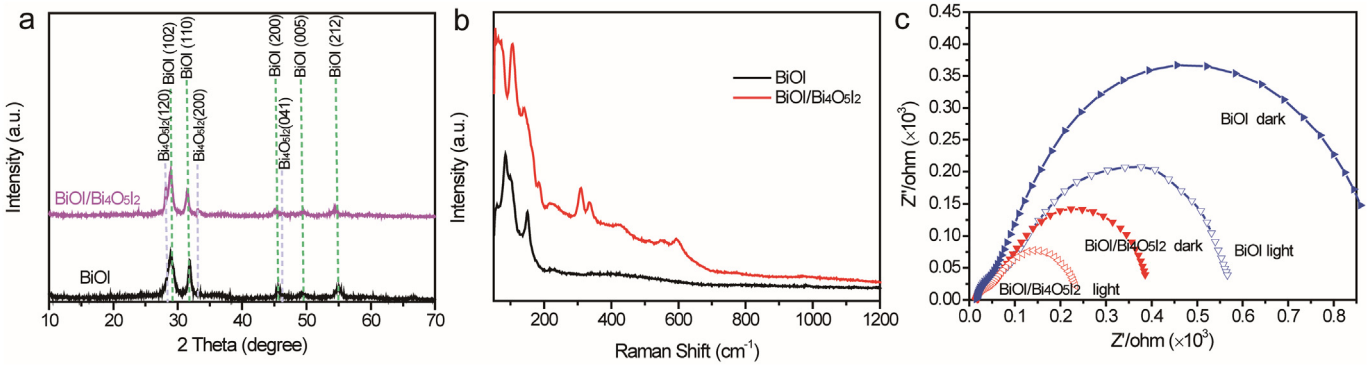

Fig. 2. (a) XRD, (b) Raman spectra and (c) EIS spectra of BiOI and BiOI/$Bi_4O_5I_2$.

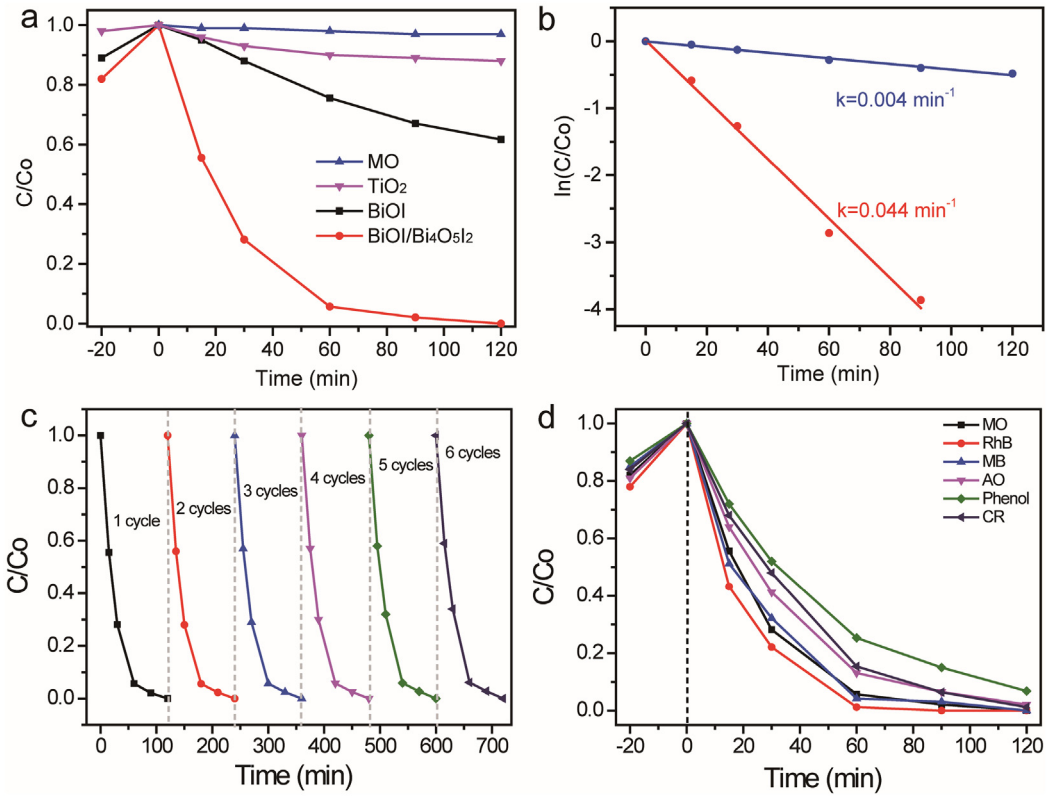

Fig. 3. (a) Photocatalytic performance and (b) pseudofirst-order reaction kinetics of BiOI, TiO_2 and BiOI/$Bi_4O_5I_2$ for degradation of MO. (c) Cycling performance of photocatalytic degradation of MO over BiOI/$Bi_4O_5I_2$. (d) Photocatalytic performance of BiOI/$Bi_4O_5I_2$ for degradation of organic pollution (MO, RhB, MB, AO, Phenol and CR) under the irradiation of visible light.

and heterojunction could promote the separation of electrons and holes.

In summary, we prepared BiOI/$Bi_4O_5I_2$ by annealing pristine BiOI at 400 °C in air. The BiOI/$Bi_4O_5I_2$ composites demonstrate 5 times higher photocatalytic activity than the pristine BiOI for MO degradation under the irradiation of visible light. Moreover, the BiOI/$Bi_4O_5I_2$ composites have superior cycling stability. Such enhanced photoactivity is due to the significantly enhanced separation efficiency of photogenerated. This work not only provides a new insight into heterojunction in promoting photocatalytic activity but also opens up new possibilities for efficient visible-light driven photocatalysts.

Acknowledgement

This work was supported by the Natural Science Foundation of China (21706295), Natural Science Foundation of Guangdong Province (2017A030313055), Young Teachers' Scientific Research and Cultivation Fund of South China Normal University (17KJ19) and the Middle School Student Talent Plan.

Appendix A. Supplementary material

Supplementary data to this article can be found online at https://doi.org/10.1016/j.inoche.2018.05.009.

References

[1] A. Khan, R. Zia ur, M.-u. Rehman, R. Khan, A. Waseem Zulfiqar, A. Iqbal, Z.H. Shah, CdS nanocapsules and nanospheres as efficient solar light-driven photocatalysts for degradation of Congo red dye, Inorg. Chem. Commun. 72 (2016) 33–41.

[2] W.-M. Liao, J.-H. Zhang, Y.-J. Hou, H.-P. Wang, M. Pan, Visible-light-driven CO_2 photo-catalytic reduction of Ru(II) and Ir(III) coordination complexes, Inorg. Chem. Commun. 73 (2016) 80–89.

[3] R. Wang, G. Cheng, Z. Dai, J. Ding, Y. Liu, R. Chen, Ionic liquid-employed synthesis of Bi_2E_3 (E = S, Se, and Te) hierarchitectures: the case of Bi_2S_3 with superior visible-light-driven Cr(VI) photoreduction capacity, Chem. Eng. J. 327 (2017) 371–386.

[4] X. Yu, J. Yang, K. Ye, X. Fu, Y. Zhu, Y. Zhang, Facile one-step synthesis of BiOCl/BiOI heterojunctions with exposed {001} facet for highly enhanced visible light photocatalytic performances, Inorg. Chem. Commun. 71 (2016) 45–49.
[5] Z. Chen, J. Liao, Y. Chen, J. Zhang, W. Fan, Y. Huang, Synthesis of oxygen deficient BiOI for photocatalytic degradation of methyl orange, Inorg. Chem. Commun. 74 (2016) 39–41.
[6] Y. Huang, K. Li, Y. Lin, Y. Tong, H. Liu, Enhanced efficiency of electron–hole separation in $Bi_2O_2CO_3$ for photocatalysis via acid treatment, ChemCatChem (2018), http://dx.doi.org/10.1002/cctc.201800101.
[7] Y. Huo, R. Hou, X. Chen, H. Yin, Y. Gao, H. Li, BiOBr visible-light photocatalytic films in a rotating disk reactor for the degradation of organics, J. Mater. Chem. A 3 (2015) 14801–14808.
[8] H. Li, J. Shang, Z. Ai, L. Zhang, Efficient visible light nitrogen fixation with BiOBr nanosheets of oxygen vacancies on the exposed {001} facets, J. Am. Chem. Soc. 137 (2015) 6393–6399.
[9] S. Wang, X. Hai, X. Ding, K. Chang, Y. Xiang, X. Meng, Z. Yang, H. Chen, J. Ye, Light-switchable oxygen vacancies in ultrafine Bi_5O_7Br nanotubes for boosting solar-driven nitrogen fixation in pure water, Adv. Mater. 29 (2017) 1701774.
[10] A. Li, T. Wang, X. Chang, W. Cai, P. Zhang, J. Zhang, J. Gong, Spatial separation of oxidation and reduction co-catalysts for efficient charge separation: Pt@TiO_2@MnOx hollow spheres for photocatalytic reactions, Chem. Sci. 7 (2016) 890–895.
[11] Y. Huang, H. Xu, H. Yang, Y. Lin, H. Liu, Y. Tong, Efficient charges separation using advanced BiOI-based hollow spheres decorated with palladium and manganese dioxide nanoparticles, ACS Sustain. Chem. Eng. 6 (2018) 2751–2757.
[12] Y. Huang, W. Fan, B. Long, H. Li, F. Zhao, Z. Liu, Y. Tong, H. Ji, Visible light Bi_2S_3/Bi_2O_3/$Bi_2O_2CO_3$ photocatalyst for effective degradation of organic pollutions, Appl. Catal. B Environ. 185 (2016) 68–76.
[13] H. Huang, K. Xiao, Y. He, T. Zhang, F. Dong, X. Du, Y. Zhang, In situ assembly of BiOI@$Bi_{12}O_{17}Cl_2$ p-n junction: charge induced unique front-lateral surfaces coupling heterostructure with high exposure of BiOI {001} active facets for robust and nonselective photocatalysis, Appl. Catal. B Environ. 199 (2016) 75–86.
[14] G. Cai, L. Xu, B. Wei, J. Che, H. Gao, W. Sun, Facile synthesis of β-Bi_2O_3/$Bi_2O_2CO_3$ nanocomposite with high visible-light photocatalytic activity, Mater. Lett. 120 (2014) 1–4.
[15] Y. Chen, Y. Guo, H. Hu, S. Wang, Y. Lin, Y. Huang, Achieving low temperature formaldehyde oxidation: a case study of $NaBH_4$ reduced cobalt oxide nanowires, Inorg. Chem. Commun. 82 (2017) 20–23.
[16] Y. Huang, H. Hu, S. Wang, M.S. Balogun, H. Ji, Y. Tong, Low concentration nitric acid facilitate rapid electron–hole separation in vacancy-rich bismuth oxyiodide for photo-thermo-synergistic oxidation of formaldehyde, Appl. Catal. B Environ. 218 (2017) 700–708.
[17] Y. Huang, H. Li, M.-S. Balogun, W. Liu, Y. Tong, X. Lu, H. Ji, Oxygen vacancy induced bismuth oxyiodide with remarkably increased visible-light absorption and superior photocatalytic performance, ACS Appl. Mater. Interfaces 6 (2014) 22920–22927.
[18] X. Xiao, C. Xing, G. He, X. Zuo, J. Nan, L. Wang, Solvothermal synthesis of novel hierarchical $Bi_4O_5I_2$ nanoflakes with highly visible light photocatalytic performance for the degradation of 4-tert-butylphenol, Appl. Catal. B Environ. 148-149 (2014) 154–163.
[19] Y. Huang, H. Li, W. Fan, F. Zhao, W. Qiu, H. Ji, Y. Tong, Defect engineering of bismuth oxyiodide by IO_3^- doping for increasing charge transport in photocatalysis, ACS Appl. Mater. Interfaces 8 (2016) 27859–27867.
[20] K. Wang, G. Zhang, J. Li, Y. Li, X. Wu, 0D/2D Z-scheme heterojunctions of bismuth tantalate quantum dots/ultrathin g-C_3N_4 nanosheets for highly efficient visible light photocatalytic degradation of antibiotics, ACS Appl. Mater. Interfaces 9 (2017) 43704–43715.
[21] K.-H. Ye, Z. Wang, H. Li, Y. Yuan, Y. Huang, W. Mai, A novel CoOOH/(Ti, C)-Fe_2O_3 nanorod photoanode for photoelectrochemical water splitting, Sci. China Mater. (2018), http://dx.doi.org/10.1007/s40843-017-9199-5.